doi:10.1093/brain/awp277 Brain 2010: 133; 33–45 | 33

BRAIN
A JOURNAL OF NEUROLOGY

Mapping interictal oscillations greater than 200 Hz recorded with intracranial macroelectrodes in human epilepsy

Benoît Crépon,[1,2,3,4] Vincent Navarro,[1,2,3,4] Dominique Hasboun,[1,2,3,4] Stéphane Clemenceau,[1,2,3,5] Jacques Martinerie,[1,2,3] Michel Baulac,[1,2,3,4] Claude Adam[1,2,3,4] and Michel Le Van Quyen[1,2,3]

1 Centre de Recherche de l'Institut du Cerveau et de la Moelle Epinière, INSERM UMRS 975, Paris, France
2 Université Pierre et Marie Curie - Paris 6, Paris, France
3 CNRS UMR 7225, Paris, France
4 Epilepsy Unit, Groupe Hospitalier Pitié-Salpêtrière Assistance Publique – Hôpitaux de Paris, France
5 Neurosurgery Department, Groupe Hospitalier Pitié-Salpêtrière, Assistance Publique – Hôpitaux de Paris, France

Correspondence to: Michel le Van Quyen,
Centre de Recherche de l'Institut du Cerveau et de la Moelle Epinière,
INSERM UMRS 975,
47 Bd de l'Hôpital,
75651 Paris Cedex 13, France
E-mail: lenalm@ext.jussieu.fr

Interictal high-frequency oscillations over 200 Hz have been recorded with microelectrodes in the seizure onset zone of epileptic patients suffering from mesial temporal lobe epilepsy. Recent work suggests that similar high-frequency oscillations can be detected in the seizure onset zone using standard diagnostic macroelectrodes. However, only a few channels were examined in these studies, so little information is available on the spatial extent of high-frequency oscillations. Here, we present data on high-frequency oscillations recorded from a larger number of intracerebral contacts spatial (mean 38) in 16 patients. Data were obtained from 1 h of interictal recording sampled at 1024 Hz and was analysed using a new semi-automatic detection procedure based on a wavelet decomposition. A detailed frequency analysis permitted a rapid and reliable discrimination of high-frequency oscillations from other high-frequency events. A total of 1932 high-frequency oscillations were detected with an average frequency of 261 ± 53 Hz, amplitude of 11.9 ± 6.7 μV and duration of 22.7 ± 11.6 ms. Records from a patient often showed several different high-frequency oscillation patterns. We classified 24 patterns from 11 patients. Usually (20/24 patterns) high-frequency oscillations were nested in an epileptic paroxysm, such as a spike or a sharp wave, and typically high-frequency oscillations (19/24) were recorded from just one recording contact. Unexpectedly in other cases, high-frequency oscillations (5/24) were detected simultaneously on two or three contacts, sometimes separated by large distances. This large spatial extent suggests that high-frequency oscillations may sometimes result from a neuronal synchrony manifest on a scale of centimetres. High-frequency oscillations were almost always recorded in seizure-generating structures of patients suffering from mesial (9/9) or polar (1/3) temporal lobe epilepsy. They were never found in the epileptic or healthy basal, lateral temporal or extra temporal neocortex nor in the healthy amygdalo–hippocampal complex. These findings confirm that the generation of oscillations at frequencies higher that 200 Hz is, at this scale, a specific, intrinsic property of seizure-generating networks in medial and polar temporal lobes, which have a common archaic phylogenetic origin. We show that this activity can be detected and its spatial extent determined with conventional intracranial electroencephalography electrodes in records from patients with temporal lobe epilepsy. It is a reliable marker of the seizure onset zone that should be considered in decisions on surgical treatment.

Received May 12, 2009. Revised September 7, 2009. Accepted September 11, 2009. Advance Access publication November 17, 2009

Keywords: high-frequency oscillations; mesial temporal lobe epilepsy; intracranial EEG; fast ripple; seizure onset zone

Abbreviations: EEG = Electroencephalography; FR = fast ripple; HFOs = high-frequency oscillations; HS = hippocampal sclerosis; MTL = mesial temporal lobe; SOZ = seizure onset zone; TF = time frequency; TP = temporal pole

Introduction

Presurgical evaluation of epilepsy patients aims to define the seizure onset zone (Engel, 1996). Long-term video EEG recording is a necessary procedure for the precise localization of this area in refractory partial epilepsies (Wyllie, 1997; Engel and Pedley, 1998). Among investigation methods for this evaluation, intracranial EEG remains the only way to record electrophysiological activity directly from brain structures and to formulate hypotheses about how they may be involved in epileptic processes (Talairach *et al*., 1974). In this context, a large number of studies have been dedicated to the analysis of the earliest EEG changes associated with seizures (Spencer *et al*., 1992). Nevertheless, interpretation of invasive ictal recordings requires that several stereotyped clinical seizures be recorded and this can prolong the time needed to several weeks. This time could be reduced if specific information permits reliable localization of the seizure onset zone from interictal markers.

Knowledge on the properties of electrophysiological signals generated by the seizure onset zone between seizures remains elusive. Brain structures involved in the seizure onset zone usually produce transient interictal spikes. However, interictal epileptic activities recorded with intracranial EEG are numerous and variable, often arising from multiple sites which are seldom discretely localized to the region of seizure onset (Alarcon *et al*., 1997). More recently, it has been suggested that interictal high-frequency oscillations (HFOs) may have a diagnostic value. In particular, fast and abnormal HFOs with frequencies in the range 180–500 Hz (fast ripples) have been recorded during interictal periods with microelectrodes from the hippocampus and entorhinal cortex of patients with mesial temporal lobe (MTL) epilepsy (Bragin *et al*., 1999, 2002*b*; Staba *et al*., 2004). Similar events are detected in rodent models of MTL epilepsy (Bragin *et al*., 2002*a*; Dzhala and Staley, 2004; Foffani *et al*., 2007). Fast ripples occur at higher frequencies in the epileptic MTL containing atrophic hippocampi and amygdala than in contralateral MTL. They provide a promising diagnostic marker for epileptic areas associated with hippocampal sclerosis and consequent synaptic reorganization (Rampp *et al*., 2006). Fast ripples may not only permit the localization of epileptic networks, but also provide insight into mechanisms of epileptogenesis (Khalilov *et al*., 2005; Le Van Quyen *et al*., 2006). However, microelectrode recordings raise concerns about patient safety and neurosurgical procedures and may provide lower quality, less stable data than can be achieved in a routine presurgical setting. Recently, Urrestarazu *et al*. (2007) convincingly showed that interictal HFOs may be detected and used to localize the seizure onset zone in intracranial records obtained from broadband depth electrodes of small size (surface area 0.9 mm^2). Using hybrid depth electrodes containing microwires and macroelectrodes, Worrell *et al*. (2008) confirmed that HFOs can be recorded in the hippocampal seizure onset zone with using standard clinical macroelectrodes (surface area 9.3 mm^2). They report that the distribution of HFO frequencies recorded with macroelectrodes falls off more rapidly than in records made with microwires and observed HFO >200 Hz only rarely. Due to the low rate of detection of HFOs using clinical macroelectrodes, the authors could not draw reliable conclusions on the spatial extent of HFOs in epileptic patients.

The present studies were designed to obtain data on this point. We asked whether HFOs were limited to a single recording site or whether they could be detected at multiple sites in a systematic analysis of multiple intracranial EEG records obtained during interictal periods. Our data were obtained from 16 consecutive patients undergoing presurgical evaluation for medically refractory focal epilepsy, with MTL or neocortical epilepsy.

Patients and methods

Patients

We studied 16 consecutive patients (eight male, mean age: 37 years) with intractable partial epilepsy requiring an exploration with intracranial electrodes between April 2002 and July 2006 at La Pitié Salpêtrière Epilepsy Unit. All patients had a comprehensive non-invasive evaluation prior to intracranial exploration, including a detailed history and neurological examination, neuropsychological testing sometimes including a intracarotid amobarbital test, brain MRI, functional nuclear neuroimaging [Positron Emission Tomography (PET) and interictal-ictal single photon emission computed tomography] and prolonged continuous scalp video-EEG recordings (Adam *et al*. 1997). All patients gave their informed consent and procedures were approved by the local ethical committee (Comité de Protection des Personnes).

Intracranial electrodes and clinical data

Records were made continuously in the video-EEG unit from each patient using intra-cranial depth electrodes and, occasionally, subdural strips (Ad-Tech Medical Instruments, Racine, WI). The insertion of depth electrodes with a Leksell frame was based on coordinates obtained from a trajectory simulation on a 3D brain MRI. Subdural strips were introduced through burr holes. Brain structures to be explored were defined from hypotheses on the seizure onset zone localization derived from non-invasive clinical evaluations (Table 1) (Adam *et al*., 1996). Depth electrodes were composed of 4–10 cylindrical contacts 2.3 mm long, 1 mm in diameter, 10 mm apart centre to centre, mounted on a 1 mm wide flexible plastic probe. Subdural electrodes were strips with four to eight one-sided circular contacts, 2.3 mm in diameter and with a centre to centre separation of 10 mm. The effective surface area was 7.2 mm^2 for depth contacts and 4.15 mm^2 for subdural contacts. The exploration of one patient

Table 1 Clinical, neuroimaging, electrophysiogical and operative data of the 16 patients

Patient	Gender/ age	Age of onset (years)	Aura	Scalp EEG SOZ	Intracranial EEG: SOZ	Ictal SPECT (hyper perfusion)	PET (hypo metabolism	MRI	Epileptogenic zone	Surgery	Neuropathology	Surgical outcome
A	F 49	12	Visceral, dysmnesic	R-T, L-T	R-Tm(3), L-Tm(1)			R-HS + Tpwgd	Bi-Tm	R-AMTR	HS	IA (3 years)
B	F 28	25	Visceral	R-T	R-Tm(3), R-Tlb(9)	R-Tmblp	R-Tbl	N	R-Tmbl	R-AMTR[a]	HS	IIIA (5 years)
C	M 41	0.3	Anxiety	R-T, L-T	R-Tm(6)	R-T, R-Fo	R-Tp	R-HS	R-Tm	R-AMTR	HS	IIA (2 years)
D	M 33	15	Dysmnesic	Bi-T	R-Tm(12)	Bi-Tmp	R-Tmp L-Tp	R-HS	R-Tm	R-AMTR	HS	IIA (1 years)
E	F 39	8	Visceral	R-T	R-Tm→Bi-T(9)			R-HS + Tpwgd	R-Tm	R-AMTR	HS	IIB (1 years)
F	M 26	16	Visceral, olfactory	L-FT	L-Tm→L-Tp(7)	Bi-Tm	L-Tm	L-H hyperintensity	L-Tm	L-AMTR	HS	IA (1 years)
G	M 39	12	No (complex seizure straightaway)	Bi-T	L-Tm(8)	Bi-Tm	Bi-Tm	L-H malrotation	L-Tm	L-AMTR	HS	IA (3 years)
H	F 43	16	Dreamy state	R-T, L-T	L-Tm(4), R-Tp(2)	L-TI	Bi-Tmp	Bi-HS	L-Tm, R-Tp			
I	M 41	17	Dysmnesic, auditory hallucinations	R-T	R-Tm(8)		R-Tmb	N	R-Tm			
J	F 33	16	Visceral	R-T, L-T	R-Tl(10), L-Tp(2)		L-Tmp	N	R-Tl, L-Tp			
K	M 39	7	No (complex seizure straightaway)	R-T	R-Tp→R-Fo(19)	R-TpI,C	R-FT	R- Tpwgd	R-Tp			
L	F 39	11	Well-being, auditory illusion	R-T	R-Tb(ant→post)(2)	R-Tm	R-Tp	N	R-Tb	R-large AMTR	Dysgenesic abnormality	IIA (3 years)
M	M 45	12	Oculocephalic version	L-TO, L-T	L-Tlpost(50)	L-Tmp	L-Tmbl	N	L-Tpost	L post T3 lobectomy[a]	Gliosis	IVB (4 years)
M′					L-Tlpost(52)							
N	F 26	10	Visual hallucination, oculocephalic version	L-TPO, L-T	L-Ob(5)		L-ObTb	N	L-Ob			
O	F 35	24	Dizzyness, visual hallucination	R-T, L-T	R-Ob(6), R-Tpost(8)			R-O dysplasia	R-Ob, R-Tpost			
P	M 35	6	Paresthesia	R-P	R-P(2)		R-TP	R-PT dysplasia	R-P	Lesionectomy	Dysplasia	IC (6 years)

Patients are named by a letter from A to P. Sex M = male; F = female. Patient M was twice implanted and included in the study. Seizure onset zone (SOZ): seizure onset zone as recorded with scalp EEG then intracranial EEG. Comma indicates multiple seizure onset zones. → indicates first propagation. Number of seizures recorded in brackets. Surgical outcome according Engel's classification (Duration of follow up in brackets). L = left; R = right; Bi = bilateral; T = temporal (m = mesial; b = basal; l = lateral; p = polar), F = frontal (I = inferior); O = occipital; P = parietal; C = cingular; I = insular; H = hippocampus. SPECT = single photon emission completed tomography; HS = hippocampal sclerosis; Tpwgd = temporal pole white-gray matter dedifferentiation; AMTR = anterior mesial temporal resection; N = normal; ant = anterior; post = posterior.

a Patients with limited resection. The whole putative epileptogenic zone was not removed to limit cognitive impairments.

Table 2 Depth electrodes implantation data

Patient #	Type of electrodes	Hippocampus recorded	Neocortex recorded	Number of contacts located in each structure					Duration of record (s)
				Amygdala/ Hippocampus	Para-hippocampal gyrus	Temporal pole	Other	Total	
A	SCo	LR	Bi-T	10	2	6	34	52	2465
B	S	R	R-T	2	1	1	16	20	3534
C	S	LR	R-F	5	2	0	25	32	3282
D	SCo	LR	Bi-T	10	0	3	43	56	3931
E	SCo	LR	Bi-T	6	0	4	40	50	3649
F	S	LR	L-T	5	1	1	32	39	4229
G	S	L	L-T	4	2	0	20	26	3455
H	SCo	LR	Bi-T	3	7	4	38	52	3247
I	S	L	L-T	3	2	0	16	21	3721
J	SCo	LR	Bi-T	7	1	6	40	54	2768
K	S	R	R-FT	3	1	1	26	31	2383
L	SCo	R	R-T	4	1	3	20	28	4586
M	S	L	L-T	3	0	0	33	36	2816
M'	S	0	L-TO	0	0	0	29	29	6306
N	S	0	L-TPO	0	0	0	34	34	2497
O	S	R	R-TlbO	4	0	0	22	26	3603
P	S	0	R-PT	0	0	0	29	29	2872
Total				69	20	29	497	615	3491

Type of electrodes. SCo = each temporal lobe is recorded with one depth hippocampal Spencer's probe and three subdural strips (for Patient L, only right temporal lobe is recorded). S = stereo EEG (depth electrodes) only. L = left; R = right; Bi = bilateral; T = temporal (m = mesial; b = basal; l = lateral; p = polar); F = frontal (I = inferior); O = occipital; P = parietal; C = cingular; I = insular; H = hippocampus.

comprised four to nine electrodes corresponding to an average of 38 contacts per patient as described in Table 2. Pre- and post-implantation MRI scans were evaluated to locate each contact anatomically and precisely along the electrode trajectory. While electrodes were inserted in different trajectories within the temporal lobe (lateral-to-medial or posterior-to-anterior), their location could always be identified in the amygdala, the hippocampal head, body and tail, or in other medial temporal lobe structures.

All seizures recorded for each patient were visually identified and reviewed. The structures where the earliest EEG changes appeared during seizure we defined as the seizure onset zone. Secondary implicated structures were defined as the first propagation zone.

Nine Patients (A–I) suffered from MTL epilepsy. Neuropathology showed hippocampal sclerosis in Patients A–G. A second independent epileptic focus was found in the ipsilateral temporal lobe for Patient B, or in the contralateral temporal pole (H). Seizures originated from the temporal neocortex in four Patients (J–M), in the occipital lobe for Patients N and O and the parietal lobe for Patient P (Table 1).

High sampling data acquisition

Intracranial EEG data were acquired with a sampling rate of 1024 Hz using a 128 channel Micromed system (16 bit, bandwidth at 3 dB: 0.1–320 Hz). Recording took place in a Faraday room and lasted ~1 h (mean 54 min). All patients were awake during recording. All data were from interictal periods occurring at least 2 h from a seizure.

Data analysis: semi-automatic detection of high-frequency oscillations

We developed a procedure to detect HFO events that consisted of an initial automatic detection followed by a visual confirmation by an observer (B.C.) who was blind to clinical data and investigative conclusions. This detection was independently performed on each electrode contact (total number: 615; Table 2).

Highly sensitive automatic detection of high-frequency oscillation events

EEG was first studied using a local bipolar montage based on the potential difference between pairs of adjacent contacts. An average reference montage was subsequently shown to locate more precisely high-frequency activity. First, after filtering data in the high-frequency range between 180 and 400 Hz (using the MATLAB Signal Processing Toolbox function 'fir2', a windowed digital Finite Impulse Response filter with a magnitude gain near one between 180 and 400 Hz and near zero below 170 Hz and above 420 Hz), the signal envelope was computed using a Hilbert transform. Then, its local maxima (corresponding to putative HFO events) were automatically detected using a threshold set to 5 standard deviations (SD) of the envelope calculated over the whole recording. This value of 5 was previously used by Staba *et al*. (2004) in HFO detection. We further confirmed the validity of this threshold by performing a sensitivity/specificity analysis, using a full visual screen of HFOs in single-channel epochs from five patients. A group of 148 HFOs, visually identified by a human reviewer (B.C.), was used as a benchmark for measuring the performance of our algorithm. The Receiver Operating Characteristic (ROC) curve showed that a 5 SD threshold was associated with a sensitivity of 100% and a specificity of 90.5% (Supplementary Fig. 1). Similar to Worrell *et al*. (2008), we selected a low specificity threshold to produce a detection procedure with high sensitivity. We compared the performance of our algorithm to that obtained from another HFO detection method (Gardner *et al*., 2007) and the results were similar (Supplementary Fig. 1).

Visual validation of high-frequency oscillation assisted by a time–frequency decomposition

This procedure detected many events, with frequent false positive ones, which were then screened visually and discarded if necessary. For this purpose, we developed a custom graphical user interface to screen candidate HFO events visually. This interface displayed the untreated signal together with two band-pass filtered signals and a time frequency map using a wavelet decomposition for frequency from 1 to 400 Hz (Le Van Quyen and Bragin, 2007). More precisely, we used a complex Morlet wavelet $w(t,f)$ with a Gaussian shape in both time and frequency domains around a central time t and frequency f: $w(t,f) = \pi^{-1/4}.e^{-t^2/2\sigma_t^2}.e^{2i\pi ft}$. A wavelet family is characterized by a constant ratio f/σ_f that we set at 10 ($\sigma_f = 1/2\pi\sigma_t$). The time–frequency map $E(t,f)$ of the signal is the square norm of the result of convolution of a complex wavelet with the signal $s(t)$: $E(t,f) = |w(t,f) \otimes s(t)|^2$. To improve visualization and contrast, all time frequency maps represent $\log[E(t,f)]$ as log (μV^2/s).

The simultaneous display of the filtered signal and its time frequency map let us select HFO events according to several criteria: (i) HFOs had to be visually detectable on the unfiltered signals as sinusoidal waves; (ii) the time–frequency map of an HFO had to show a primary peak in the frequency range 180–400 Hz. Indeed, artefactual high-frequency activities can be caused by harmonics of lower frequency activities or by sharp components of epileptiform discharges that usually induce a broadband increase in the high-frequency range that obscured HFO detection (Supplementary Fig. 2). Thus, we excluded broad-band high-frequency activities related to isolated spikes, but retained narrow-band HFOs with sufficient amplitudes (above 8 SD), even if they co-occurred with a spike; and (iii) rare high-frequency events, occurring less than once every 10 min, were retained only if they recurred on a similar EEG background (for example, at the same phase of a sharp wave or simultaneous to a paroxysm on a nearby contact; Supplementary Fig. 3).

Quantification of high-frequency oscillation

Each selected HFO event was quantified by: (i) the amplitude of the HFO (μV) defined by the local maximum of the envelope; (ii) the duration of the event (ms) defined by the time for which the envelope around the event remained above the half of the threshold, or 2.5 times the SD; and (iii) the maximum of the time frequency map in the frequency band of interest defined by the power (μV^2) and the modal frequency (Hz) of the HFO. Calculations and analyses were computed using MATLAB 7.3 software (The Mathworks Inc., Massachusetts).

Results

High-frequency oscillations detection and quantification

We identified HFOs in the intracranial EEG recordings of sixteen patients using the two steps procedure. About 185 000 candidate events were detected automatically and 1932 HFOs were selected from these by visual inspection and time–frequency analysis. These selected HFOs all had a circumscribed power increase in the high-frequency range. Typical examples of HFOs from the hippocampus are shown, with their corresponding time–frequency decomposition, in Fig. 1. Histograms of all detected HFOs sorted by frequency show a primary peak near 240 Hz (Fig. 2). The mean frequency of all selected events was 261 ± 53 Hz (median 250 Hz), the mean amplitude was 11.9 ± 6.7 μV (median 10.1 μV) and mean duration was 22.7 ± 11.6 ms (i.e. 8.7 oscillations, median 20 ms). They occurred at a rate of 1.6 per min. About 95% of HFOs were nested within a spike or a sharp wave, typically just after the maximal deflexion. For a given recording contact, the HFO always occurred at the same phase of the paroxysm. In two patients (see Patient A of Fig. 1), these sharp-wave HFO complexes occurred periodically every 1 to 2 s. In Patient C, HFOs co-occurred at the same contact with lower frequency oscillations (100–200 Hz).

Spatial and temporal extension of high-frequency oscillations

For each patient, HFOs were classed into distinct patterns based on their anatomic location, EEG morphology, the simultaneous occurrence of a paroxysm, frequency and their spatial extent. When a HFO was recorded simultaneously on several contacts within 10 ms, its spatial extent was defined by the number of involved contacts and its location was defined by the maximal amplitude. These features permitted the separation of several different HFO patterns (range 1–5) for each patient (Table 3). Most HFO patterns (19/24) were limited to a single recording contact (Fig. 3A). We note that the associated sharp waves typically had a larger spatial extent and were observed on several nearby contacts (Fig. 4A). In five of 24 patterns, HFOs were detected on two or three contacts, sometimes quite distant (Fig. 4B). Anatomically, 18 patterns were recorded from the amygdala or hippocampus (in all patients, 69 contacts were located in these structures; Table 2 and Fig. 3B), four in parahippocampal gyrus (20 contacts) and 2 in temporal polar cortex (29 contacts), whereas no HFOs were observed in extra temporal or temporal lateral neocortex (497 contacts). For 11 patterns (Patients C, D and G), different HFOs followed each other in time with a latency of more than 10 ms, suggesting a propagation phenomenon. Figure 5 shows an example of HFOs nested in interictal sharp waves generated in the body of right hippocampus (Patient D, patterns D1 and D2). Another HFO of similar frequency, duration and amplitude range, was recorded 24 ms later on the next contact, in the tail of the hippocampus (patterns D3 and D4 gathered). Finally, a ripple oscillation in the 100–200 Hz band was recorded in the head of the hippocampus. We detected two patterns of propagation in this case: sometimes the ripple temporally surrounded the HFO in the body of hippocampus (pattern D2 in the body followed by D4 in the tail), or the ripple followed it (pattern D1 in the body followed by D3 in the tail).

In another example, from Patient G, 77 similar HFOs were associated with a spike-and wave (pattern G1) recorded in the head of left hippocampus. Sometimes (41/77) a small, slower

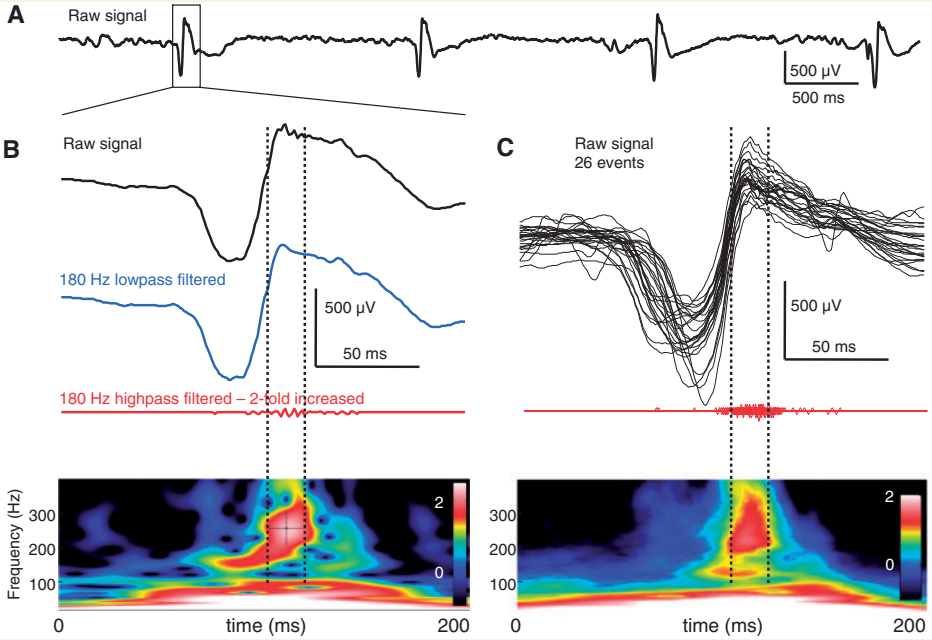

Figure 1 Representative examples of interictal HFOs recorded at the head-body junction of a sclerotic hippocampus (Patient A, pattern A1). (**A**) Six seconds of raw intracranial EEG. HFOs are nested in sharp waves which appear periodically every 1.5 s. (**B**) Top: expanded traces of the first sharp wave. The HFO can be seen in the raw signal just after the maximal deflexion of the wave. It is not visible in a standard EEG record sampled at 400 Hz (blue, low-pass filtered signal). Bottom: the time–frequency map of the HFO. The power of the oscillation is depicted by a colour scale code. The time–frequency map provides information on the stability of oscillation frequency with time and on the spread of frequencies involved (black cross). (**C**) Top: expanded traces of 26 similar HFOs. Bottom: mean time–frequency map of all recorded events.

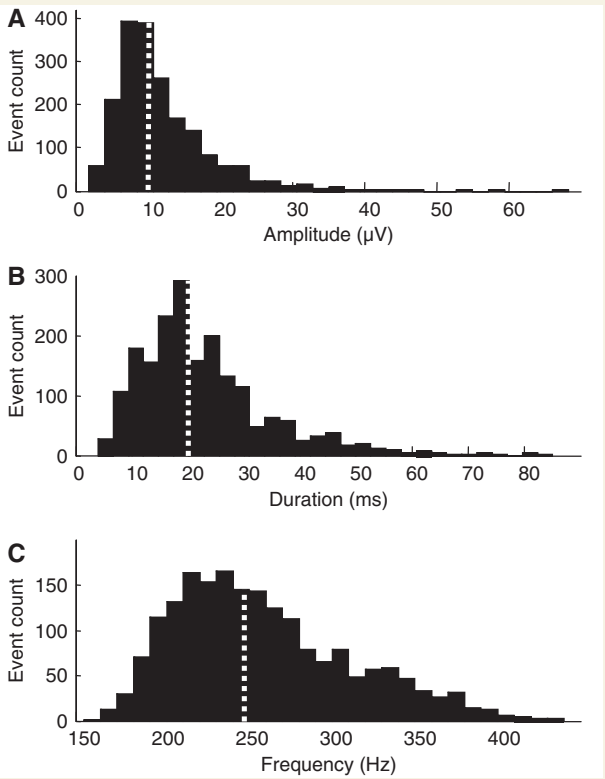

Figure 2 Histograms of all selected HFOs ($n = 1932$) sorted by amplitude (**A**), duration (**B**) and frequency (**C**). The white dotted line indicates the median.

HFO was recorded on the same contact 85 ms before (pattern G3). Often (64/77), the G1–HFO was followed by a slower HFO on the last contact of the next electrode in the head of the hippocampus (pattern G2).

Correlation between high-frequency oscillations and the seizure onset zone

For each of the nine patients suffering from MTL epilepsy (A to I, Table 4), HFOs were generated in the seizure onset zone (16 patterns), or in the first propagation zone (Patient A). Figure 6 summarizes the exploration of Patient A: HFOs were recorded in one contact of the head of the hippocampus during a 41′ interictal period. They predicted the seizure onset zone precisely and more rapidly than analysis of complex EEG records of several weeks of interictal and ictal epileptic activities. HFOs were detected unilaterally in five of seven patients in which both hippocampi were recorded. They were usually recorded in the seizure onset zone (10/13 contacts, Table 4), or in first propagation sites (6/16 contacts). Three patterns were detected at other sites in two patients with bi-temporal HFOs: for Patient C, HFOs were recorded in both hippocampi, whereas seizures were detected only in the right one. The pattern C5 was recorded in left hippocampus where no seizure emerged during the invasive evaluation. Nevertheless, previous non-invasive evaluations had shown that seizures could emerge from both temporal lobes asynchronously. The pattern C3 was recorded in the tail of right hippocampus, not considered as seizure onset zone, but patterns C1 and C2,

Table 3 Summary of selected HFO patterns

No.	Location	Count	Rate min^{-1}	Frequency (Hz) mean (SD)	Amplitude (μV) mean (SD)	Duration (ms) mean (SD)	Spatio-temporal remarks
A1	Head–body junction R hippocampus	38	0.92	264 (43)	16.4 (3.8)	19.5 (7.7)	
B1	Head of R hippocampus	115	1.95	228 (30)	7.7 (1.7)	23.9 (6.9)	AVI next white matter
B2	Tail of R hippocampus	165	2.8	250 (28)	10.7 (3.4)	20.4 (8.6)	
C1	Depth of R collateral sulcus	57	1.04	251 (36)	9.6 (3)	21 (8.3)	AVI R amygdala and tail of hippocampus
C2	Depth of R collateral sulcus	34	0.62	278 (20)	6.1 (1.5)	29 (11)	AVI R amygdala and tail of hippocampus
C3	R amygdala–lateral basal	19	0.35	226 (26)	2.8 (0.9)	24.7 (4.7)	50 ms before C1
C4	Tail of R hippocampus	9	0.16	236 (12)	2.4 (0.5)	25.7 (7.9)	100 ms before C2
C5	L amygdala–hippocampus junction	66	1.21	288 (42)	10.1 (2.8)	17.4 (7.7)	
D1	Body of R hippocampus	62	0.89	329 (28)	8.2 (2.9)	21.2 (13)	
D2	Body of R hippocampus	71	1.13	324 (35)	6.8 (1.6)	22.1 (14)	
D3	Tail of R hippocampus	62	0.96	324 (39)	7.8 (2)	31.7 (14)	24 ms after D1
D4	Tail of R hippocampus	71	1.08	314 (44)	6.7 (1.6)	25.5 (16)	24 ms after D2
E1	R entorhinal cortex	315	5.18	219 (27)	10.4 (3.3)	20.7 (4.5)	AVI R amygdala and head of hippocampus
F1	Head of L hippocampus	33	0.47	276 (43)	5.3 (1.4)	16.6 (3.2)	AVI inferior circular sulcus of insula
G1	Head of L hippocampus	77	1.34	309 (52)	16.1 (6.2)	17.9 (13)	
G2	Body of L hippocampus	64	1.11	267 (35)	18.4 (6.9)	18.5 (12)	12 ms after G1 (same sharp wave)
G3	Head of L hippocampus	41	0.71	244 (24)	4.4 (6.6)	22.9 (15)	85 ms before G1
G4	Head of L hippocampus	62	1.08	249 (25)	7 (1.8)	23.7 (7.8)	
H1	L entorhinal cortex–near amygdala	241	4.45	222 (27)	15.2 (7.3)	22.1 (11)	
H2	L temporal pole–lateral	116	2.14	296 (51)	14.1 (6.1)	17.4 (12)	
H3	R temporal pole–medial	30	0.55	259 (35)	2.7 (0.6)	20.3 (7)	
I1	L amygdala–hippocampus junction	281	4.53	238 (34)	16.7 (8.7)	21.7 (13)	
J1	Head of L hippocampus	132	2.86	355 (39)	13.4 (9.3)	17.3 (14)	
K1	Head of R hippocampus	13	0.33	242 (30)	18.1 (9.1)	24.7 (13)	
	Mean		1.58	270 (33)	9.9 (3.9)	21.9 (10)	

For each patient, HFOs were categorized in different patterns based on anatomic location, EEG morphology, frequency and spatial extent. If a HFO was simultaneously recorded on several contacts, its location was defined by the maximal amplitude, with secondary locations described in last column.
L = left; R = right; AVI = also visible in. SD = standard deviation.

recorded in the seizure onset zone, were also visible in the tail. In the case of Patient H, with a bi-temporal epilepsy, HFOs were detected in both independent seizure onset zones: left entorhinal cortex (pattern H1) and right temporal pole (pattern H3). HFOs were also recorded in the left temporal pole (pattern H2), where electrical stimulation typically provoked left temporal seizures.

For two patients, whose seizures were initiated just in the temporal pole (Patients J and K; Tables 3 and 4), HFOs were only recorded in the ipsilateral hippocampus. The seizure onset zone of Patient L was localized to the anterior basal temporal by intracranial EEG, but this electrode was no longer available when the interictal recording for HFOs were made. In this patient, no HFOs were detected, even though medial structures were implicated secondarily in ictal events. Finally, no HFOs were detected, either in neocortex or in mesiotemporal structures, for four Patients (M–P) suffering from extra-temporal (1 parietal, 2 occipital) or lateral temporal epilepsies.

Discussion

Three main findings were obtained in this study. First, we confirmed that HFOs between 180 and 400 Hz can be detected in interictal periods with standard, large-sized intracranial macroelectrodes. Secondly, while HFOs were generally limited to a single contact, confirming a local spatial extent, they could be recorded from up to three contacts, suggestive of a larger neural network. Thirdly, HFOs were mostly recorded in the seizure onset zone for each of the nine patients suffering from MTL epilepsy. In contrast, they were never found outside the mesiotemporal structures or in the healthy amygdala or hippocampus. Specifically HFOs were not detected in patients suffering from neocortical epilepsy, suggesting that they may be useful in routine invasive presurgical localization of MTL epileptic foci.

Submillimetre high-frequency oscillations >200 Hz recorded with macroelectrodes

Discrete fast ripple oscillations in the range of 250–500 Hz were first described in human with microelectrodes that record a local field potential from a volume of around 1 mm^3 (Bragin *et al.*, 1999). More recently, using larger depth macroelectrodes (0.8 mm^2), HFOs were visually identified close to seizures (Jirsch *et al.*, 2006) or associated with interictal spikes (Urrestarazu *et al.*, 2007). Finally, interictal HFOs have been recorded with

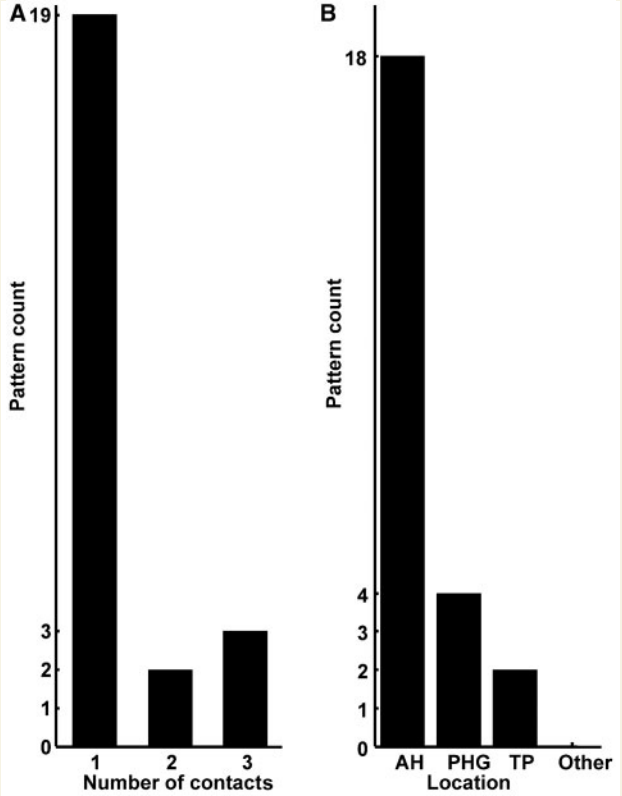

Figure 3 Spatial extent and location of the 24 HFO patterns. (**A**) Histogram of HFO spatial extent, defined by the number of contacts expressing, within a 10 ms time lag, a high-frequency activity in selected HFO patterns. In most cases (19 patterns out of 24), HFOs were recorded from a single contact. In other patterns, HFOs were detected nearly simultaneously on two or three contacts. (**B**) Anatomic location of HFO patterns. In most cases (18 patterns out of 24), HFOs were recorded in the amygdalo-hippocampal (AH) complex. Four cases were observed in parahippocampal gyrus (PHG) and two other cases in the temporal pole (TP). No HFOs were recorded in lateral or basal temporal cortex or in locations outside the temporal lobe.

conventional macroelectrodes of contact area greater than 1 mm^2, which presumably record the activity of 100 mm^3 of brain tissue (Worrell *et al*., 2008). Our study confirms that HFOs can be detected when signals from conventional intracranial EEG macroelectrodes are recorded at a high sampling rate (1024 Hz). These HFOs have similar properties in terms of frequency, amplitude and duration to those recorded with microelectrodes, they are also nested within sharp wave and their localization is similar. On the basis of these observations, we postulate that focal HFOs reflect the same local, highly synchronous oscillations as those recorded with microelectrodes. This conclusion is supported by the co-occurrence of interictal fast ripples and HFOs in simultaneous records made with microwires and macroelectrodes (Worrell *et al*., 2008).

Furthermore, we detected distinct HFOs with novel spatiotemporal properties that occurred nearly simultaneously on several EEG channels. Interictal HFOs were, for 5/24 patterns, recorded from two or three contacts (with a separation of 10 mm between adjacent contacts on the same electrode). Our data suggest that networks that generate HFOs or through which they propagate can extend over volumes of cm^3. These HFOs presumably reflect synchronization of distant neuronal structures since we sometimes recorded HFOs on three contacts with those of the middle electrode having the smallest amplitude (Fig. 4B, pattern E1). These pathological hypersynchronies contrast with physiological oscillations where the oscillation frequency is negatively correlated with its amplitude, reflecting the volume of the generator network according to a *1/f* relation (Penttonen and Buzsáki, 2003; Buzsáki and Draguhn, 2004). In contrast, for 11/24 patterns, HFOs followed a reproducible spatiotemporal sequence. This implies several interconnected networks that can both oscillate at high frequency and also initiate similar oscillations in nearby structures; presumably as occurs during seizure initiation. This interictal activity may then provide insights into dynamic processes that initiate a seizure. Future studies should compare these interictal patterns with high frequency synchronizations at seizure onset.

Conventional intracranial EEG can thus effectively detect and characterize HFOs at frequencies above 180 Hz. Microelectrodes detect activity from a volume limited to usually emerging at the distal end of the macroelectrodes. Compared with microelectrodes, macroelectrodes may permit detection of HFOs within a larger brain volume and so provide a better understanding of the propagation of this high-frequency epileptic activity. Furthermore, our use of standard intracranial electrodes permitted systematic and simultaneous mapping of multiple cortical sites, providing an original large-scale analysis of HFOs during the interictal period.

A strategy to detect high-frequency oscillations

Even with presently available electrode, amplifier and high-sampling data acquisition technology, HFOs are hard to detect since their signal-to-noise ratio is low and they rarely occur at one or a few recording sites. We feel that a visual detection of HFOs, using digital techniques alone to examine long-term records, may be impossible. While EEG screens typically display between 5 and 20 s of data, a 300 ms window might be most appropriate for the visual detection of HFOs (Schevon *et al*., 2004). A close, visual reading of an interictal EEG with a 300 ms per screen display for each of the recorded channels becomes time-consuming and tiring. In our study of 16 patients, a mean recording duration of 54 min represents 10^6 windows of 250 ms. At one window per second, this analysis would take 4 months, night and day. Thus, reliable automated methods seem to be obligatory to localize and track HFOs in long-term records. Nevertheless, the construction of a fully automated HFOs detection system is not easy. The EEG signal is non-stationary and both the variation in background activity and presence of

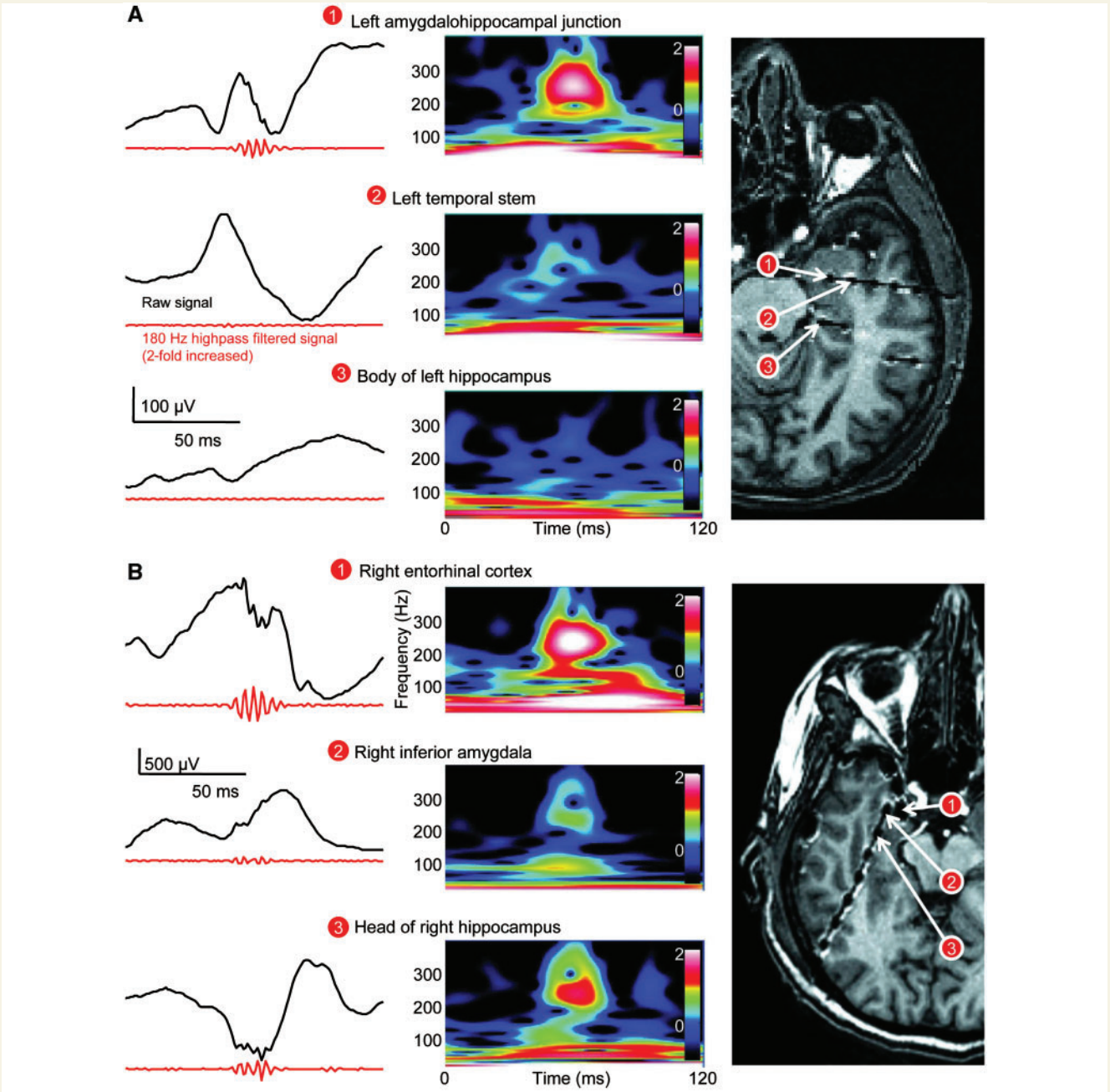

Figure 4 (**A**) A typical local HFO recorded from one contact at the left amygdalo-hippocampal junction (Top, Pattern I1). Note the HFO is nested in a sharp wave which is detected without a HFO in two adjacent contacts (middle–bottom). (**B**) A representative example of a HFO recorded from three contacts. Its amplitude is maximal in an electrode recording from entorhinal cortex (subdural strip). Note that the HFO amplitude is minimal at contact 2, situated between contacts 1 and 3, suggesting a long-range synchronization phenomenon rather than simple diffusion.

EEG paroxysms complicate automated analyses (Liu *et al*., 2002). Sudden variations, including epileptic spikes, have a wide band spectrum and by producing high-frequency artefacts in filtered data can lead to false detections by automatic algorithms. Furthermore, while there is a consensus on the identification of paroxysms like sharp waves (Gotman, 1980), no consensus exists for HFOs. In particular, HFO morphology varies with distance from their site of generation, leading to an imprecise, operator-dependant characterization. We therefore developed a semi-automatic detection strategy that reduced the need for human supervision and overcame some difficulties associated with the use of automated methods on single-channel data. Our highly

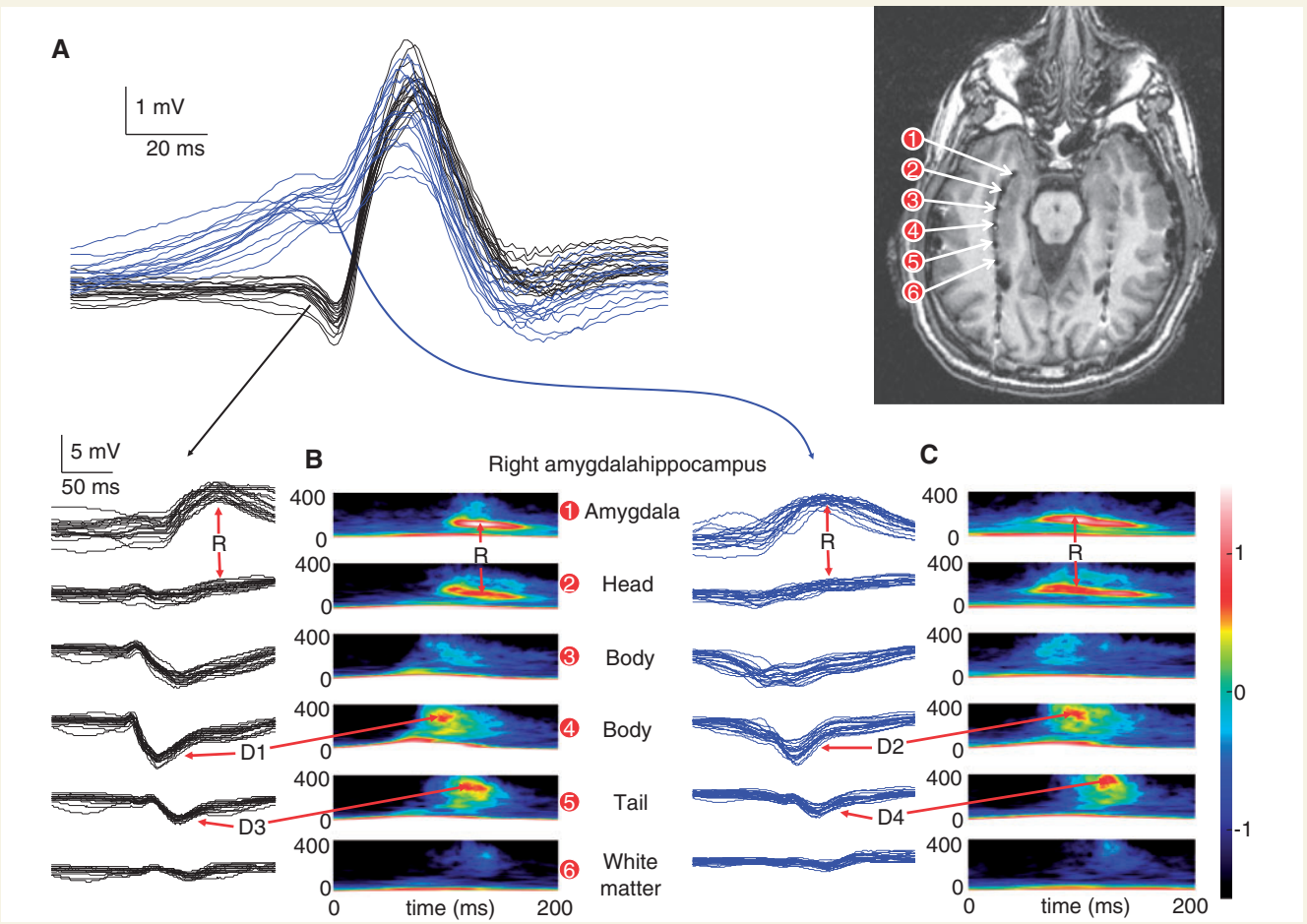

Figure 5 (**A**) Thirty-six consecutive HFOs (out of 133) recorded from the body of a sclerotic hippocampus (Patient D) are aligned with inflexion of the nested sharp wave (bipolar montage, contact 3–4. For localization, see MRI). Two types of events with distinct spatiotemporal patterns (17 and 19 events, respectively) can be distinguished (patterns D1 in black and D2 in blue). (**B** and **C**) Left: spatial extent of events recorded from the right hippocampus (referential versus average montage) for each pattern. Right: mean time frequency map of each pattern of HFOs. The sharp wave was detected throughout the amygdalo hippocampus complex. A sharp wave and HFO in tail of hippocampus (contact 5, patterns D3 and D4; see arrows) occurs 24 ms after a similar complex in the body (contact 4, patterns D1 and D2). While a HFO nested with a slower 130 Hz HFO (R) sometimes occurs after (**B**) (19 events out of 36, patterns D1) and sometimes before (**C**) (17 events out of 36, patterns D2).

sensitive automatic detection paradigm generated many false positive events which were then screened and discarded by visual review. The custom graphical user interface we developed to screen candidate HFO events displays short-time windows containing raw signals, band-pass filtered signals and time–frequency decompositions. The wavelet decomposition tool works as a 'mathematical microscope' to dissect the instantaneous frequency content of signal and enhance detection of short-duration low-amplitude activities that are often masked by high-amplitude, low-frequency and large-scale integrated EEG activity (Le Van Quyen and Bragin, 2007).

If HFO events can be used as a more specific index of a seizure onset zone than epileptic spikes, then it will be necessary to distinguish them reliably from high-frequency components of epileptic spikes. We attempted to resolve this essential issue by imposing strict criteria for positive detection including the presence of HFO in the raw EEG signal, a reproducibility of HFO form and the presence of two separate maxima in time–frequency analyses, one for HFO and another for the nested epileptic paroxysm.

High-frequency oscillations as a marker of mesial temporal lobe epilepsy: clinical relevance

For the nine patients with MTL epilepsy, HFOs were always recorded in the seizure-generating structures. The spatial properties and frequency content of these HFOs are similar to those

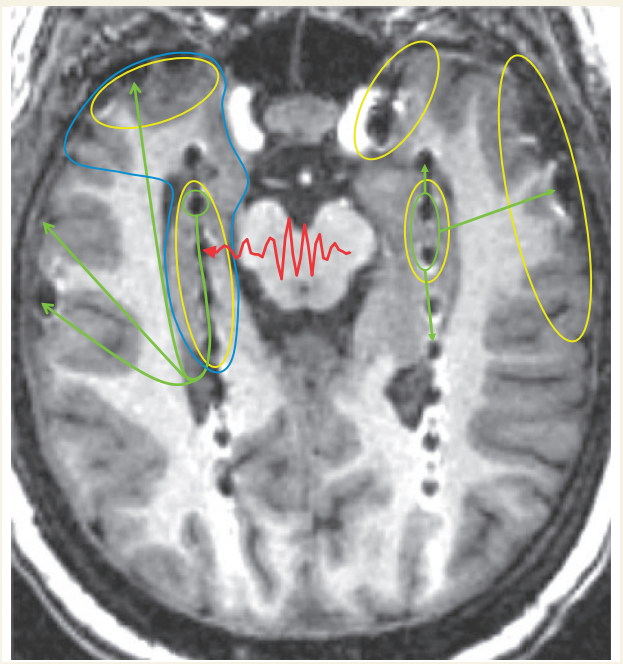

Figure 6 Comparison of seizure onset zone (green), irritative zone (yellow), epileptogenic zone (blue) and interictal HFO zone (red) in Patient A. Scalp EEG showed asynchronous bi-temporal interictal ictal activities. Bi-temporal intracranial EEG recorded three complex partial seizures (emerging from the head of the right hippocampus, spreading along hippocampus, then to right temporal neocortex and finally propagating to left temporal lobe) and one aura (emerging from left temporal lobe with maximum amplitude in anterior part of hippocampus). Interictal asynchronous spikes were recorded in right hippocampus and both temporal poles, and synchronous spikes in left hippocampus and lateral temporal cortex. Patient is seizure free 3 years after resection of right amygdala, hippocampus and anterior temporal lobe (blue curve). Interictal HFOs around 260 Hz were recorded only in the head–body junction of the right hippocampus (red arrow).

recorded from limbic epileptic structures with microelectrodes in patients with MTL epilepsy (Bragin *et al*., 1999, 2002*b*; Staba *et al*., 2004) as well as in excitotoxic models such as kainate-induced epilepsy in rodents (Bragin *et al*., 2002*a*). These findings suggest that events specific to MTL epilepsy produce neural networks that can generate hypersynchronous, high-frequency activity (>200 Hz). They may involve the synaptic reorganization that is known to occur during secondary epileptogenic processes (Bragin *et al*., 2004; Khalilov *et al*. 2005, Le Van Quyen *et al*., 2006). HFOs of a similar frequency content, around 240 Hz, have also been identified in patients just before seizure onset at sites close to seizure initiation (Jirsch *et al*., 2006) as well as in animal models of hippocampal seizures (Traub *et al*., 2001; Khalilov *et al*. 2005; Khosravani *et al*., 2005). In contrast, seizures arising from neocortical structures have been shown to begin with lower-frequency fast oscillations in the gamma range 30–100 Hz (Allen *et al*., 1992; Alarcon *et al*., 1995; Worrell *et al*., 2004). This suggests that neuronal networks specific to an epileptic mesial temporal cortex produce hypersynchronous events at frequencies above 200 Hz not only between seizures but also at seizure onset. Thus HFOs may be a specific marker of the mesial temporal seizure onset zone in patients with MTL epilepsy (Bragin *et al*., 1999, 2002*b*; Staba *et al*., 2004; Urrestarazu *et al*. 2007; Worrell *et al*., 2008). In five of the patients examined in this study, scalp EEG records showed a bi-temporal asynchronous or simultaneous seizure onset. In each case, interictal HFO localization was concordant with the site of seizure onset in mesial temporal limbic structures. Patient A was particularly interesting: seizures were initiated independently in both hippocampi; surgery of right hippocampus, where HFOs took place, cured the epilepsy (Fig. 6). Of the seven neuropathologically proven cases of hippocampal sclerosis, three had a typical MRI and one had radiological hyperintensity without atrophy. In all cases, HFOs were observed in the amygdo–hippocampal complex. This suggests that HFOs provide a good sensitivity for the identification of hippocampal sclerosis.

In five patients with neocortical epilepsies, HFOs were not detected either in epileptic structures or in healthy regions of neo or medial temporal cortex. These results seem to imply that neocortical epileptic networks do not generate HFOs, which appears to contradict other recent studies (Jacobs *et al*. 2008, 2009). A possible reason for these differences may result from the nature of the epileptic syndrome. In our patients, no lesions were detected by MRI, while a heterotopia or dysplasia was identified in the previously mentioned studies. Another reason may be the electrode size. HFOs were first recorded with micro electrodes, then with electrodes with infra millimetric active surface area, but less easily with the larger contacts (Worell *et al*. 2008). The absence of HFOs in mesial temporal limbic structures in three neocortical patients confirms their negative predictive value for seizure onset zone detection in hippocampus.

The temporal poles seems to represent a special entity. In one patient, a seizure onset zone was associated with HFOs whereas HFOs were present only in ipsilateral hippocampus for two others. This suggests that mesocortex of temporal pole or parahippocampal gyrus, as well as the archeocortex of amygdala or hippocampus, can generate such activity. In two patients with seizure onsets in the temporal pole, the presence of HFOs in ipsilateral hippocampus opens questions on the involvement of temporal limbic structures in the epileptic network or their modifications by frequent, early ictal propagation from the pole (Kahane *et al*., 2002).

In conclusion, interictal HFOs >200 Hz can be recorded with macroelectrodes. They seem to provide useful additional evidence for diagnostic analysis of intracranial EEG data. When present in temporal polar epilepsies, they either reinforce a suspected polar location or question whether hippocampal structures are involved in a larger epileptic network. HFOs in cases of medial temporal limbic epilepsies confirm the location of the seizure onsets, may suggest a stronger implication of the parahippocampal gyrus and

Table 4 Locations of HFOs versus seizure onset/early propagation zones for Patients A–K

Patient	Seizure onset zone	First propagation zone	HFOs recorded elsewhere
A	1. Head of R hippocampus	*Head–body junction of R hippocampus*	
	2. Head and body of L hippocampus	Tail of L hippocampus	
B	*1. Head of R hippocampus*	Tail of R hippocampus, T3 neocortex depth of R superior temporal sulcus	
	2. T2 neocortex (basal anterior)	T1 neocortex	
C	*Depth of R collateral sulcus*	T2 neocortex *R amygdala—lateral basal*	*L amygdala–hippocampus junction* *Tail of R hippocampus*
D	*Body of R hippocampus*	*Tail of R hippocampus*	
	R amygdala	Head of R hippocampus	
E	*Right inferior amygdale* *Head of R hippocampus*	*R entorhinal cortex*	
F	*Head of L hippocampus*	*L amygdala—lateral basal*	
G	*Body of L hippocampus*	*Head of L hippocampus* Depth of R collateral sulcus	
H	*1. R temporal pole—medial* Depth of R collateral sulcus	R orbital gyrus—lateral R orbital gyrus—posterior	
	2. Head of L hippocampus L entorhinal cortex	L amygdala—lateral basal L temporal pole—medial	*L temporal pole—lateral*
I	*L amygdale–hippocampus junction*	L insulae	
J	1. L temporal pole	*Head of L hippocampus*	
	2. R temporal pole		
K	R temporal pole	*Head of R hippocampus* T1 neocortex	

HFO locations are indicated in italics. Note that, in most of the cases, HFOs were detected within the seizure onset zone. Independent seizure onset zones are indicated for patients A, B, H and J by numbers 1 and 2.

could help discriminate the 'worst' hippocampus to be surgically removed. Finally, the absence of HFOs in neocortical epilepsies further emphasizes that the hippocampus is unlikely to be involved in seizure onset.

Acknowledgements

The authors thank Richard Miles for helpful comments on the manuscript and Laurent Hugueville for technical assistance with the EEG amplification system.

Funding

This work was supported by the European Union-FP7 Project EPILEPSIAE (Evolving Platform for Improving Living Expectation of Patients Suffering from IctAl Events, Grant No 211713). B.C. was supported by INSERM.

Supplementary material

Supplementary material is available at *Brain* online.

References

Adam C, Clemenceau S, Semah F, Hasboun D, Samson S, Aboujaoude N, et al. Variability of presentation in medial temporal lobe epilepsy: a study of 30 operated cases. Acta Neurol Scand 1996; 94: 1–11.

Adam C, Clémenceau S, Semah F, Hasboun D, Samson S, Dormont D, et al. Strategy of evaluation and surgical results in medial temporal lobe epilepsy. Rev Neurol (Paris) 1997; 153: 641–651.

Alarcon G, Binnie CD, Elwes RD, Polkey CE. Power spectrum and intracranial EEG patterns at seizure onset in partial epilepsy. Electroencephalogr Clin Neurophysiol 1995; 94: 326–337.

Alarcon G, Seoane JJG, Binnie CD, Miguel MCM, Juler J, Polkey CE, et al. Origin and propagation of interictal discharges in the acute electrocorticogram. Implications for pathophysiology and surgical treatment of temporal lobe epilepsy. Brain 1997; 120: 2259–2282.

Allen PJ, Fish DR, Smith SJ. Very high-frequency rhythmic activity during SEEG suppression in frontal lobe epilepsy. Electroencephalogr Clin Neurophysiol 1992; 82: 155–159.

Bragin A, Engel J, Wilson CL, Fried I, Buzsáki G. High-frequency oscillations in human brain. Hippocampus 1999; 9: 137–142.

Bragin A, Mody I, Wilson CL, Engel J. Local generation of fast ripples in epileptic brain. J Neurosci 2002; 22: 2012–2021.

Bragin A, Wilson CL, Almajano J, Mody I, Engel J. High-frequency oscillations after status epilepticus: epileptogenesis and seizure genesis. Epilepsia 2004; 45: 1017–1023.

Bragin A, Wilson CL, Staba RJ, Reddick M, Fried I, Engel J. Interictal high-frequency oscillations (80-500 Hz) in the human epileptic brain: entorhinal cortex. Ann Neurol 2002; 52: 407–415.

Buzsáki G, Draguhn A. Neuronal oscillations in cortical networks. Science 2004; 304: 1926–1929.

Draguhn A, Traub RD, Bibbig A, Schmitz D. Ripple (approximately 200-Hz) oscillations in temporal structures. J Clin Neurophysiol 2000; 17: 361–376.

Dzhala VI, Staley KJ. Mechanisms of fast ripples in the hippocampus. J Neurosci 2004; 24: 8896–8906.

Engel J. Surgery for seizures. N Engl J Med 1996; 334: 647–652.

Engel J, Pedley T, editors. Epilepsy: A Comprehensive Textbook. New York: Lippincott-Raven; 1998.

Foffani G, Uzcategui YG, Gal B, de la Prida LM. Reduced spike-timing reliability correlates with the emergence of fast ripples in the rat epileptic hippocampus. Neuron 2007; 55: 930–941.

Gardner AB, Worrell GA, Marsh E, Dlugos D, Litt B. Human and automated detection of high-frequency oscillations in clinical intracranial EEG recordings. Clin Neurophysiol 2007; 118: 1134–1143.

Gotman J. Quantitative measurements of epileptic spike morphology in the human EEG. Electroencephalogr Clin Neurophysiol 1980; 48: 551–557.

Jacobs J, LeVan P, Chander R, Hall J, Dubeau F, Gotman J. Interictal high-frequency oscillations (80-500 Hz) are an indicator of seizure onset areas independent of spikes in the human epileptic brain. Epilepsia 2008; 49: 1893–1907.

Jacobs J, Levan P, Châtillon C-É, Olivier A, Dubeau F, Gotman J. High frequency oscillations in intracranial EEGs mark epileptogenicity rather than lesion type. Brain 2009; 132: 1022–37.

Jirsch JD, Urrestarazu E, LeVan P, Olivier A, Dubeau F, Gotman J. High-frequency oscillations during human focal seizures. Brain 2006; 129: 1593–1608.

Kahane P, Chabardès S, Minotti L, Hoffmann D, Benabid A-L, Munari C. The role of the temporal pole in the genesis of temporal lobe seizures. Epileptic Disord 2002; 4: S51–S58.

Khalilov I, Le Van Quyen M, Gozlan H, Ben-Ari Y. Epileptogenic actions of GABA and fast oscillations in the developing hippocampus. Neuron 2005; 48: 787–796.

Khosravani H, Pinnegar CR, Mitchell JR, Bardakjian BL, Federico P, Carlen PL. Increased high-frequency oscillations precede in vitro low-Mg seizures. Epilepsia 2005; 46: 1188–1197.

Le Van Quyen M, Bragin A. Analysis of dynamic brain oscillations: methodological advances. Trends Neurosci 2007; 30: 365–373.

Le Van Quyen M, Khalilov I, Ben-Ari Y. The dark side of high-frequency oscillations in the developing brain. Trends Neurosci 2006; 29: 419–427.

Liu HS, Zhang T, Yang FS. A multistage, multimethod approach for automatic detection and classification of epileptiform EEG. IEEE Trans Biomed Eng 2002; 49: 1557–1566.

Penttonen M, Buzsáki G. Natural logarithmic relationship between brain oscillators. Thalamus and Related Systems 2003; 48: 1–8.

Rampp S, Stefan H. Fast activity as a surrogate marker of epileptic network function? Clin Neurophysiol 2006; 117: 2111–2117.

Schevon CA, Thompson T, Hirsch LJ, Emerson RG. Inadequacy of standard screen resolution for localization of seizures recorded from intracranial electrodes. Epilepsia 2004; 45: 1453–1458.

Spencer SS, Guimaraes P, Katz A, Kim J, Spencer D. Morphological patterns of seizures recorded intracranially. Epilepsia 1992; 33: 537–545.

Staba RJ, Wilson CL, Bragin A, Jhung D, Fried I, Engel J. High-frequency oscillations recorded in human medial temporal lobe during sleep. Ann Neurol 2004; 56: 108–115.

Talairach J, Bancaud J, Szikla G, Bonis A, Geier S, Vedrenne C. [New approach to the neurosurgery of epilepsy. Stereotaxic methodology and therapeutic results. 1. Introduction and history] Neurochirurgie 1974; 20: 1–240.

Traub RD, Whittington MA, Buhl EH, LeBeau FE, Bibbig A, Boyd S, Cross H, Baldeweg T. A possible role for gap junctions in generation of very fast EEG oscillations preceding the onset of, and perhaps initiating, seizures. Epilepsia 2001; 42: 153–170.

Urrestarazu E, Chander R, Dubeau F, Gotman J. Interictal high-frequency oscillations (100-500 Hz) in the intracerebral EEG of epileptic patients. Brain 2007; 130: 2354–2366.

Urrestarazu E, Jirsch JD, LeVan P, Hall J, Avoli M, Dubeau F, et al. High-frequency intracerebral EEG activity (100-500 Hz) following interictal spikes. Epilepsia 2006; 47: 1465–1476.

Wyllie E. edn. The treatment of epilepsy: Principles and practice. 2nd edn., Baltimore: Williams & Wilkins; 1997.

Worrell GA, Gardner AB, Stead SM, Hu S, Goerss S, Cascino GJ, Meyer FB, Marsh R, Litt B. High-frequency oscillations in human temporal lobe: simultaneous microwire and clinical macroelectrode recordings. Brain 2008; 131: 928–937.

Worrell GA, Parish L, Cranstoun SD, Jonas R, Baltuch G, Litt B. High-frequency oscillations and seizure generation in neocortical epilepsy. Brain 2004; 127: 1496–1506.